Cryogenic Thermal Mask for Space-cold Optical Testing for Space Optical Systems

Dae Wook Kim[1*] and James H. Burge[1]

[1]*College of Optical Sciences, University of Arizona, 1630 E. University Blvd, Tucson, Arizona 85721, USA*
[*]*Corresponding author: letter2dwk@hotmail.com*

Abstract: An optical testing configuration utilizing the Cryogenic Thermal Mask (CTM) provides thermal decoupling between a cryogenic optical system under test and a collimator operating at ambient temperature, while passing the test wavefront without significant degradation.

OCIS codes: (120.4800) Optical standards and testing; (120.6085) Space instrumentation

1. Introduction

For a space optical system, the system needs to be tested inside a space-like vacuum chamber which simulates the actual working environment of the system in space. A collimator is usually placed in the vacuum chamber to provide an ideal test beam with plane wavefront. Then, by measuring the wavefront after the test beam passes through the optical system, we can evaluate the performance of the optical system.

The temperature of the space optical system should be controlled to its working temperature during the test. For an example, the JWST primary mirror, which is designed to observe the infrared light from distant stars and galaxies, has to be kept extremely cold (*i.e.* ~40K) [1]. Thus, for the cryogenic thermal control, any heat transfer to the optical system needs to be blocked. There is no convectional thermal transfer inside vacuum. We can carefully isolate the optical system to minimize the heat transfer through conduction. Thermal radiation must be controlled to minimize thermal effects in both the cryogenic system under test and the ambient collimator.

Because the collimator directly looks at the optical system in the vacuum chamber as shown in Fig. 1, the thermal radiation from the collimator becomes a critical issue for the cryogenic thermal control. The best option may be using a collimator operating at the same temperature as the space optical system. However, making a customized cryogenic collimator will increase the total budget and project time significantly. Thus, it is highly desired to use an existing collimator such as LOTIS 6.5m collimator [2] designed to operate at certain temperature (*e.g.* ~292K).

We suggest a new testing configuration using the Cryogenic Thermal Mask (CTM) to block the thermal transfer from the collimator to the optical system while the test beam wavefront gets only small phase errors by passing through the CTM. The theoretical concept for the CTM is given in Section 2. Monte Carlo simulation results to demonstrate the feasibility of the concept are presented in Section 3.

2. Conceptual optical testing configuration using CTM

2.1 Schematic testing configuration using CTM inside a vacuum chamber

A schematic testing configuration using the CTM inside vacuum chamber is depicted in Fig. 1 (left). The CTM consist of number of consecutive thermal plates with an array of holes as shown in Fig. 1 (right). The temperature of each thermal plate is independently controlled to gradually match the temperature difference between the ambient collimator space and the space-cold optical system space.

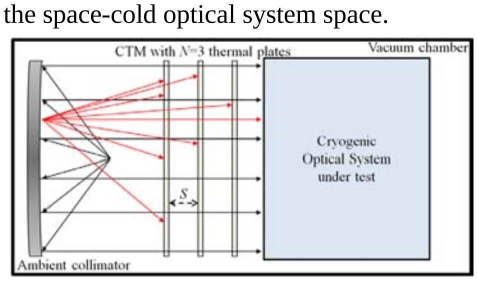

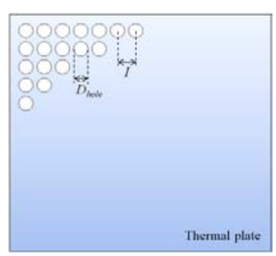

Fig. 1. Conceptual testing configuration using the CTM (left) and front view of a thermal plate with array of holes (right)

A point source reflected by the large collimator provides a collimated test beam (black rays in Fig. 1). The test beam propagates through the CTM, and be fed into the space optical system under test. However, most of the thermal radiations (red rays in Fig. 1) will be blocked by the CTM.

There are total six CTM parameters. Four of them determine the shape of the CTM as shown in Fig. 1; i) *N*: Number of thermal plates, ii) *S*: Spacing between the thermal plates, iii) D_{hole}: hole diameter, and iv) *I*: Interval between holes. Also, as other two parameters, we can control the temperature T and emissivity ε of the thermal plates. By optimizing these parameters for a given optical testing task, one can balance alignment tolerances with performance and achieve a good wavefront measurement while the thermal transfer to the optical system is minimized.

2.2 Thermal transfer control using CTM

Thermal transfer between plates is limited by the relatively small area encompassed by the holes. Using only 3 plates, the thermal transfer can be reduced to a negligible level. The thermal transfer from the ambient collimator to the space-cold optical system can be simplified and modeled as a problem with number of graybodies in the vacuum chamber as shown in Fig. 2.

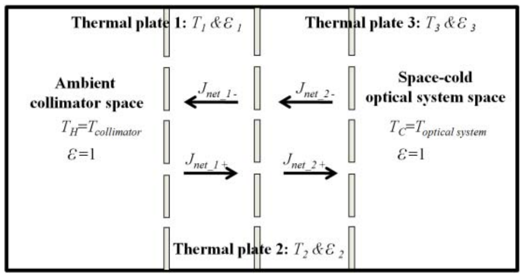

Fig. 2. Schematic thermal transfer between the thermal plates

The collimator space and the optical system space can be represented by two blackbodies with their operating temperatures T_H and T_C. The thermal plates are graybodies with given temperatures $T_{1\text{-}3}$ and emissivity $\varepsilon_{1\text{-}3}$ values. Then, the emissive power J from the graybodies can be calculated using Stefan-Boltzmann law

$$J = \varepsilon \cdot \sigma \cdot T^4 \ \ [W/m^2] \tag{1}$$

where ε is the emissivity, σ is the Stefan-Boltzmann constant: 5.67x10^{-8} $W/m^2/K^4$, and T is the absolute temperature of the graybody. Then, the total emissive power in to the cold optical system space can be minimized by changing the temperature, emissivity and geometry of the thermal plates (*e.g.* size of the holes).

Preliminary analysis of the thermal performance looks promising for isolating a 30K system from a 300K collimator. A three plate system with holes occupying 1% of the thermal plate area and with polished intermediate plate at ~250K will cause thermal loading less than 300mW/m^2 for both the ambient and the cryogenic sides of the system. More detailed calculation will be given in a separated paper [3].

2.3 Point spread function (PSF) with CTM

The collimated test beam wavefront is passed through the system via diffraction from the holes, which are carefully lined up. The nominal (*i.e.* without CTM) PSF for a space optical system with a circular stop will be a well-known Airy disk pattern in Fig. 3 (left). The angular size of Airy disk D_{Airy} is

$$D_{Airy} = 2 \cdot \lambda / D \tag{2}$$

where λ is the wavelength and D is the overall diameter of the system. However, as shown in Fig. 3 (right), the PSF with the CTM in the vacuum chamber (*i.e.* PSF_{CTM}) looks like an array of many nominal PSFs with angular spacing

$$K = \lambda / I \tag{3}$$

where I is the interval between holes, and λ is the wavelength. These are the diffraction orders due to the CTM.

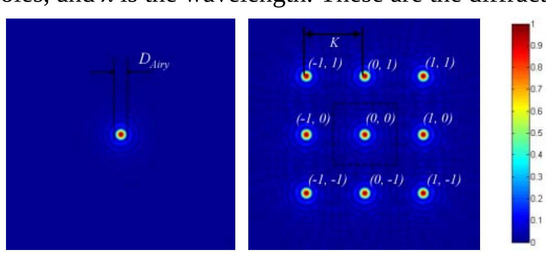

Fig. 3. Normalized nominal PSF (left) and the first nine diffraction orders of the PSF with CTM (right)

By choosing a pattern with many holes across the diameter (*e.g.* $I < D/100$), the different orders of diffraction will be spaced by many Airy pattern diameters, and will not interfere. Then, the (0, 0) order can be filtered out by putting a spatial filter at the focal plane. In this manner, the nominal wavefront can be retrieved for any following wavefront measurement. It may also be possible to use the other orders for testing field effects, but we have not modeled the sensitivity of these orders to errors in the system.

3. Induced phase error in test wavefront due to CTM tolerance

The wavefront itself will suffer errors due to imperfect hole diameter and spacing. Monte Carlo simulation was performed to demonstrate the feasibility of the optical testing with the CTM. A typical parameter values (*e.g.* D_{hole}=2mm) were used in the simulation. The wavelength λ was assumed as 1μm.

Because a manufactured real CTM will have variations in mechanical dimensions such as hole diameter and hole location, there will be wavefront error (*i.e.* phase error) due to the wave propagation through the holes in the thermal plates. A comparison between an ideal case and a realistic case is given as an example in Table 1. The distorted complex field is clearly observed as a result of the misalignments and hole diameter changes.

Table 1. Comparison between ideal and perturbed complex field in a hole at the last thermal plate [a]

Normalized amplitude map		Normalized phase map		
Perfect case	Perturbed case	Perfect case	Perturbed case	
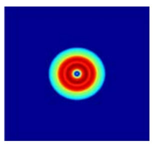	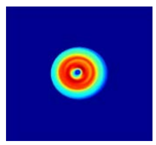	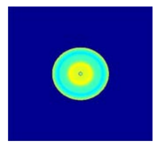	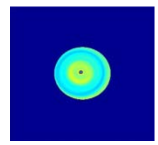	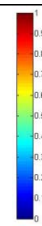

[a] Tolerance: δx = ±50 μm, δy = ±50 μm, and δD_{hole} = ±10 μm

Monte Carlo simulation for the wave propagation through the holes was performed while the alignment of the holes was perturbed up to δx and δy. At the same time, the hole diameters, D_{hole}, were also perturbed up to δD_{hole}. Then, we defined the phase error Δ_p to quantitatively asses the phase error due to the tolerance as

$$\Delta_p \equiv \{phase\ angle\ of\ \iint_{hole} U_{hole\_perturbed}(x,y)\,dx \cdot dy - phase\ angle\ of\ \iint_{hole} U_{hole\_perfect}(x,y)\,dx \cdot dy\} / 2 \cdot \pi\ \ [waves]. \tag{4}$$

The phase error was studied as a function of tolerances, δx, δy, and δD_{hole}. Same magnitude for all three tolerances was used in the simulation. The standard deviation of the phase error (error bars in Fig. 4) increase as there are more and more tolerance errors. For instance, as shown in Fig. 4, the induced RMS (Root-mean-square) phase uncertainty due to the imperfect (*i.e.* ±100 (μm) tolerance) CTM was ~±0.008 waves right after a hole in the last thermal plate. Even though this phase error varies as the CTM parameter values change, a given target wavefront accuracy for a specific testing task can be optimized and achieved in this manner.

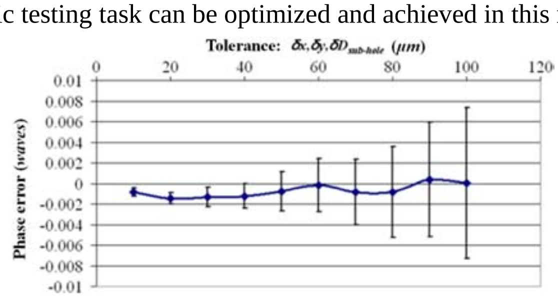

Fig. 4. Phase error vs. tolerance: Average phase error (diamond) with standard deviation (error bar).

4. Concluding remarks

The conceptual testing configuration using the CTM to test a space-cold optical system inside a vacuum chamber was introduced and the feasibility of the configuration was demonstrated based on a Monte Carlo error analysis. The thermal transfer from the ambient collimator to the space-cold optical system can be minimized while the wavefront phase error due to the CTM is still very small (*e.g.* ~±0.008 waves RMS).

5. References

[1] Mark Clampin, “Status of the James Webb Space Telescope (JWST),” in Proc. SPIE **7010**, 70100L1-7 (2008).

[2] S. C. West, S. H. Bailey, J. H. Burge, B. Cuerden, J. Hagen, H. M. Martin, and M. Tuell, “Wavefront Control of the Large Optics Test and Integration Site (LOTIS) 6.5m Collimator,” Appl. Opt. (to be published).

[3] Dae Wook Kim and James H. Burge, “Cryogenic Thermal Mask for Space-cold Optical Testing Configuration,” Opt. Express (to be submitted).